Mutagenesis Advance Access published September 1, 2012
Mutagenesis
doi:10.1093/mutage/ges046

Silver nanoparticles induce premutagenic DNA oxidation that can be prevented by phytochemicals from *Gentiana asclepiadea*

Alexandra Hudecová[1,2], Barbara Kusznierewicz[3], Elise Rundén-Pran[1], Zuzana Magdolenová[1], Katarína Hašplová[1,2], Alessandra Rinna[1], Lise Marie Fjellsbø[1], Marcin Kruszewski[4,5], Anna Lankoff[5,6], Wiggo Johan Sandberg[7], Magne Refsnes[7], Tonje Skuland[7], Per Schwarze[7], Gunnar Brunborg[8], Magnar Bjøras[9], Andrew Collins[10], Eva Miadoková[2], Eliška Gálová[2] and Mária Dušinská[1,*]

[1]Health Effects Group, NILU, P.O. Box 100, 2027, Kjeller, Norway, [2]Department of Genetics, Faculty of Natural Sciences, Comenius University, Mlynská dolina, 842 15, Bratislava, Slovakia, [3]Department of Food Chemistry, Technology and Biotechnology, Gdańsk University of Technology, Narutowicza 11/12, 80-233 Gdańsk, Poland, [4]Centre for Radiobiology and Biological Dosimetry, Institute of Nuclear Chemistry and Technology, Dorodna 16, 03-195 Warszawa, Poland, [5]Institute of Rural Health, Jaczewskiego 2, 20-090 Lublin, Poland, [6]Department of Radiobiology and Immunology, Institute of Biology, Jan Kochanowski University, Świętokrzyska 15, Kielce, Poland, [7]Department of Air Pollution and Noise and [8]Department of Chemical Toxicology, Norwegian Institute of Public Health, 0403 Oslo, Norway, [9]Centre for Molecular Biology and Neuroscience, Institute of Medical Microbiology, Rikshospitalet, 0027 Oslo, Norway, [10]Department of Nutrition, Faculty of Medicine, University of Oslo, 0316 Oslo, Norway

*To whom correspondence should be addressed. Health Effects Group, NILU, P.O. Box 100, 2027, Kjeller, Norway. Tel: +47 63 898 157; Fax: +47 63 898 050; Email: mdu@nilu.no

Received on September 16, 2011; revised on September 19, 2011; accepted June 20, 2012

Among nanomaterials, silver nanoparticles (AgNPs) have the broadest and most commercial applications due to their antibacterial properties, highlighting the need for exploring their potential toxicity and underlying mechanisms of action. Our main aim was to investigate whether AgNPs exert toxicity by inducing oxidative damage to DNA in human kidney HEK 293 cells. In addition, we tested whether this damage could be counteracted by plant extracts containing phytochemicals such as swertiamarin, mangiferin and homoorientin with high antioxidant abilities. We show that AgNPs (20 nm) are taken up by cells and localised in vacuoles and cytoplasm. Exposure to 1, 25 or 100 µg/ml AgNPs leads to a significant dose-dependent increase in oxidised DNA base lesions (8-oxo-7,8-dihydroguanine or 8-oxoG) detected by the comet assay after incubation of nucleoids with 8-oxoG DNA glycosylase. Oxidised DNA base lesions and strand breaks caused by AgNPs were diminished by aqueous and methanolic extracts from both haulm and flower of *Gentiana asclepiadea*.

Introduction

'Nanotechnology' is a rapidly expanding field, and it has had significant impacts on both therapeutic and diagnostic development over the past three decades (1). Nanomaterials are defined as substances with at least one dimension <100 nm in size, whereas the term nanoparticles (NPs) is suggested only for materials with all three external dimensions in the nanoscale (2). Nanomaterials can be found in spherical, tubular, rod- and wire-like forms, and as complex structures described as nano-onions and nanopeapods (3,4). Though numerous literature reports describe the enormous utility of these materials, knowledge about the safety of nanomaterials, their impact on cells, tissues and organs, and potential hazards to health is relatively limited (5). The small size of nanomaterials means that they readily penetrate cell and nuclear membranes; within the nucleus they may cause direct DNA damage. Nanomaterials accumulated in the cytoplasm may pose a significant genotoxic threat to DNA during mitosis. In addition, indirect oxidative damage to DNA may occur if nanomaterials induce an inflammatory response with accompanying oxidative stress (6).

Of all the nanomaterials widely used in consumer products, silver NPs (AgNPs) currently have the highest degree of commercialization (7). On account of their antimicrobial properties they have been exploited in e.g. nanofiber mats (8), bandages, wound dressings, ointments (9) and also clothing (10). Humans are continuously exposed to AgNPs from many different sources (11). Despite the escalating use of AgNPs in different industries, including nanomedicine, there is a serious lack of information, validated by scientific experiments, concerning their toxicity and the cellular responses they induce. AgNPs may express their toxicity through induction of reactive oxygen species (ROS), the level of ROS depending on the chemistry and structure of the NPs (12). The generation of ROS in the cells may result in the formation of, among other lesions, 8-oxo-7,8-dihydroguanine (8-oxoG) in DNA. Due to mispairing with adenine during replication, 8-oxoG is highly mutagenic and thus potentially carcinogenic (13).

Plants in the family *Gentianaceae* are widely used in many countries for stimulation of appetite and gastric secretion, gastroduodenal and liver protection and antifungal treatment (14). *Gentiana asclepiadea* belongs to the largest genus of the family with over 300 species (15). Its root has traditionally been used as medicine for hepatitis A virus infections (16). A wide spectrum of classes of compounds occurs in these plants, including iridoids, xanthones and C-glucoflavones. We have already shown that H_2O_2-induced damage is decreased by preincubation of cells with *Gentiana* plant extracts (17). Our aim here was to investigate whether AgNPs induce DNA base oxidation in cultured human HEK 293 cells, using the comet assay (single cell gel electrophoresis) with the lesion-specific enzyme 8-oxoG DNA glycosylase (hOGG1) to convert 8-oxoG to strand breaks (SBs). Further we were interested in whether phytochemicals present in *G. asclepiadea* plant extracts can prevent AgNP-induced DNA damage.

Materials and methods

Dispersion of AgNPs

AgNPs of nominal size 20 nm were purchased from Plasmachem GmbH, Germany.

A stock solution at 2 mg/ml was prepared just before use in filtered distilled water, vortexed and sonicated (Labsonic P, Sartorius Stedim Biotech, Goettingen, Germany) for 3 min (100% cycle, 100 watts) on ice. Immediately after sonication, phosphate-buffered saline (PBS) was added with bovine serum albumin (BSA) at a final concentration of 1.5%. BSA is commonly used for the dispersion of AgNPs as a part of a standard procedure preventing agglomeration

(18). Three concentrations of AgNPs (1 µg/ml, 25 µg/ml and 100 µg/ml) were prepared in Dulbecco's modified essential medium (DMEM) with 10% of fetal serum and added to the cells for 30 min at 37°C in a 5% CO_2 atmosphere.

Size distributions and zeta potential measurements by dynamic light scattering

Dynamic light scattering (DLS) measures multiple angles of light scatter and derives a bulk intensity plot of particle sizes. DLS was performed at 25°C with a scattering angle of 90° on the Zetasizer Nano ZS (Malvern, Malvern Hills, UK). Stock solutions were diluted to 100 µg/ml and measured in distilled water as well as in DMEM immediately and after 30 min.

Zeta potential measurements for surface charge were performed at 25°C in a folded capillary cell at 40 V using a monodispersion procedure run on the Zetasizer Nano ZS. Zeta potentials were calculated using the Smoluchowski limit for the Henry equation with a setting calculated for practical use ($f(ka) = 1.5$).

Transmission and scanning electron microscopy

The morphology of AgNPs was examined by scanning electron microscopy (SEM) in the secondary electron mode (type DSM 942, Zeiss, Germany) and transmission electron microscopy (TEM) (Jeol JEM-1220 TEM with CD camera SIS Morada 11 megapixels). For SEM analysis the sample was prepared directly on the microscope holder by placing the drop of suspension, spreading it and drying it at room temperature. Then the sample was coated with a thin layer of Au (about 10 nm), using a vacuum evaporator (JEE-4X, JEOL, Japan) to protect the sample from heat destruction and to maintain real structural parameters. It operated with an ultimate pressure of 6×10^{-4} Pa, with rotating and tilting specimen stage at a high voltage of 5 kV and working distance of 8 mm. For TEM analysis the sample was prepared on a copper mesh covered with a carbon film as the carrier.

Cell line

HEK 293 cells are originally derived from human embryonic kidney (HEK) cells grown in tissue culture. Embryonic kidneys are a heterogeneous mixture of almost all the types of cells present in the body although most cells are endothelial, epithelial or fibroblasts. HEK 293 cells are easy to grow and have been widely used in cell biology research for many years. We selected this cell line as a representative kidney model. The cells were cultured in DMEM supplemented with 10% fetal calf serum, 100 U/ml penicillin and 100 µg/ml streptomycin.

Treatment of cells with AgNPs

Pretreated and untreated cells in 12-well plates were incubated with 1, 25 or 100 µg/ml of AgNPs for 30 min in complete DMEM at 37°C in a 5% CO_2 atmosphere. Cells were then trypsinised and used in the comet assay (with or without incubation with hOGG1).

Uptake of AgNPs

Cells treated with 25 and 100 µg/ml AgNPs for 30 min in a culture flask were washed and fixed in paraformaldehyde (PFD) as follows: 4% PFD (10 min), 8% PFD (20 min, 4°C). Cells were then scraped unidirectionally, collected in a microcentrifuge tube and centrifuged (500×*g*, 10 min; 100×*g*, 2 min; 2000×*g*, 2 min; 4000×*g*, 2 min; 8000×*g*, 2 min; 12000×*g*, 5 min). Eight percent PFD was removed and 1% PFD was added. Embedding in Durcapan (epoxy resin) for electron microscopy (EM) followed: fixed cells were rinsed 3× in 0.1M sodium phosphate buffer NaPi (pH 7.4), afterwards left in 1% OsO_4 for 45 min and rinsed 3× in 0.1M NaPi (pH 7.4). Samples were serially dehydrated in ethanol 50%, 70%, 80%, 96% (15 min) and 100% ethanol (3 × 20 min). Propylenoxide was applied for 2 × 5 min, and the fixed material was transferred to porcelain trays which were then filled with Durcupan. After 30 min at 56°C, the resin was removed, fresh Durcupan was added and the samples were left overnight at room temperature. The samples were then put in capsules and polymerised at 56°C for 48 h. Resin-embedded cells were sectioned at 80 nm and transferred to 300-mesh nickel grids. Thereafter the sections were counterstained with uranyl acetate followed by lead citrate. The sections were examined in a TEM (Tecnai 12, FEI), and images were obtained with a Veleta camera.

Preparation of extracts from G. asclepiadea and treatment

G. asclepiadea plants were harvested from the Garden of Medicinal Plants, Faculty of Pharmacy, Comenius University, Bratislava. The air-dried separated plant material, weighing about 60 g, was cut into small pieces and extracted with 150 ml of methanol or water at 65°C. This procedure was repeated 5 times. The hot solution of the extract was then filtered and concentrated using a vacuum rotatory evaporator. The rest of the water was removed by azeotropic distillation with toluene and benzene using the vacuum rotatory evaporator. The final extracts (haulm methanolic, haulm aqueous, flower methanolic and flower aqueous) were kept in the dark at 4°C until tested. Cells were treated for 24 hours with 0.25, 0.5, 2.5, 5 and 25 mg/ml of *G. asclepiadea* extracts on 6-well plates.

HPLC-DAD-MS analyses of the G. asclepiadea extracts

High-performance liquid chromatography (HPLC), followed by diode array detection (DAD) and mass spectrometry (MS), was performed using an Agilent 1200 Series system. The mass spectrometer (quadrupole analyser) was equipped with an electrospray ionization interface (6130 ESI, Agilent). Chromatographic separation was carried out using an Agilent Eclipse XDB-C8 column (4.6 × 150 mm, 3.5 µm). The phytochemical resolution was carried out using a mobile phase composed of 4.8% formic acid in water (solvent A) and methanol (solvent B) at a flow rate of 1 ml/min; the injection volume of all samples was 5 µl. Elution was conducted with a linear gradient program to ensure the following ratio of solvent B to A: from 0 to 30 min (15:85 – 70:30 v/v). Absorbance spectra were recorded between 190 and 700 nm every 2 s with a bandwidth of 4 nm, while the chromatograms were monitored at 260 and 325 nm. MS parameters were as follows: capillary voltage, 3000 V; fragmentor, 120 V; drying gas temperature, 350°C; gas flow (N_2), 12 l/min; nebuliser pressure, 35 psig. The instrument was operated in positive and negative ion mode, scanning from m/z 100 to 1000. Individual compounds were identified by comparing their retention times and spectra with those for standards (swertiamarin, gentiopicroside, homoorientin, sweroside, isovitexin purchased from LGC Standards) or on the basis of available literature data and ultraviolet and mass spectra.

Trypan blue exclusion assay

Cells were trypsinised, 10 µl of cell suspension was mixed with 10-µl trypan blue (0.4%) and cell membrane integrity (percentage of unstained cells) was measured using an automated cell counter (Countess™, Invitrogen). Two experiments were performed, each with duplicates.

Clonogenic assay—colony forming ability

HEK cells (2.5×10^5) were plated on 6-well plates and incubated at 37°C in a 5% CO_2 atmosphere. After 24 hours, the cells were exposed to 0.25, 0.5, 2.5, 5 and 25 mg/ml of the plant extracts for 24 hours or to AgNPs (1, 25 and 100 µg/ml) for 30 min. After the treatment, the cells were plated on 6-well plates (200 cells per well) and cultured for 10 days. Then the cells were stained with methylene blue (1% solution), and the number of colonies was counted. The percentage colony forming ability (CFA) (relative to untreated control) was calculated.

Proliferation assay—relative cell growth activity

The cells were plated on 6-well plates (2.5×10^5) or 12-well plates (1.5×10^5) and incubated at 37°C. After 24 hours, the cells were exposed to the extracts for 24 hours or to AgNPs for 30 min and counted every 24 hours. The relative cell growth activity (RGA) was determined as the percentage increase in cell number between 0 and 96 hours.

Human 8-oxoG DNA glycosylase

Repair enzyme hOGG1 was produced at the Institute of Medical Microbiology, Norway. The purified extract (0.5 µg/µl) was diluted in buffer F (40 mM 4-(2-hydroxyethyl)-1-piperazineethanesulfonic acid (HEPES), 0.1 M KCl, 0.5 mM ethylenediaminetetraacetic acid (EDTA) and 0.2 mg/ml BSA, pH 8.0) 1:10000 just before use (19).

The comet assay

DNA damage was measured using the alkaline comet assay as described (20). Briefly, pretreated, untreated and treated cells were suspended in 1% low melting point agarose in PBS. Sixty microlitres of this suspension (approximately 2×10^4 cells) was placed on precoated slides. Slides (two for each sample) were placed in a lysis solution (2.5 M NaCl, 100 mM Na_2EDTA, 10 mM Tris–HCl, pH 10 and 1% Triton X-100) for 1 h at 4°C. After lysis the slides were either incubated with hOGG1 (50 µl/gel, 30 min, 37°C humidified atmosphere) or with a buffer or they were directly transferred to an electrophoresis tank containing an electrophoresis solution (0.3 M NaOH, 1 mM Na_2EDTA, pH > 13) for 20 min at 4°C before electrophoresis at 25 V for 30 min. The slides were then neutralised in PBS (10 min) and ddH_2O (10 min) at 4°C and stained with 20 µl SYBR® Gold nucleic acid gel stain (Invitrogen) (0.1 µl of stock per ml of TE buffer—10 mM Tris–HCl, 1 mM EDTA, pH 7.5-8). One hundred comets per sample (50 per gel) were scored by image analysis (Comet Assay IV 4.2, Perceptive Instruments Ltd), and results were expressed as % of total DNA fluorescence in tail. Cells treated with hydrogen peroxide (250 µM, 5 min, on ice) or the photosensitiser Ro19-8022 plus visible light (1 µM in PBS, 5 min, on

ice) were used as positive controls. Three to six experiments with duplicate cell samples were performed. Net hOGG1-sensitive sites (representing 8-oxoG) were estimated by subtracting % tail DNA after buffer incubation from % tail DNA after incubation with hOGG1.

Statistical analysis

The results represent the means of at least 3 experiments ± standard deviation. The distribution of data was tested by analysis of variance (ANOVA). As data were normally distributed, the significance of differences between means was evaluated by Student's *t*-test at the significance level $P < 0.05$.

Results

Characterization of AgNPs

The hydrodynamic diameter of the AgNPs was measured by DLS measurements in water and DMEM. Data are presented in Figure 1. In water, two populations of particles were detected. Most of the particles occurred as medium agglomerates with a mean diameter of 313.9 nm, and a lesser amount as large agglomerates, with a mean diameter of 3760 nm. Just after dispersion, three populations of particles were detected in DMEM, indicating single particles with mean diameter of 33.9 nm and medium and large agglomerates with mean diameter of 225.9 and 4050 nm, respectively. Most of the particles occurred as medium agglomerates. The DLS values in DMEM were also measured after incubation for 30 min and showed only a slight shift with time (Figure 1). For the single particles and the medium agglomerates we have also included the peak where most of the particles occur. These values were 164.9 nm in water, 190.1 in DMEM (just after dispersion) and 190.1 in DMEM after 30 min. This illustrates, in particular for water, the difference between the mean size and the size where most particles occurred. The z-averages for all the peaks are also presented in the table. The z-potential of the AgNPs measured in water at 100 µg/ml was −37.4 ± 2.5 mV (without BSA and PBS supplement) and −26.7 ± 0.8 mV (with BSA and PBS supplement). AgNPs were further characterised by using SEM and TEM. Figure 2 presents a SEM image showing AgNPs forming small agglomerates with average size of about 100 nm and a TEM image showing AgNPs ranging in size between 20 and 100 nm. These findings are consistent with the DLS results.

Uptake of AgNPs by HEK 293 cells

The cells were exposed to 25 or 100 µg/ml of AgNPs (20 nm) for 30 min, and intracellular and subcellular localization was analysed by TEM (Figure 3). AgNPs were clearly taken up by HEK 293 cells. NPs were visible mainly as single NPs (size from 25 to 100 nm) and were distributed mostly in the vacuoles (Figure 3a–f) and in the cytoplasm (Figure 3a–f). Pretreatment of cells with haulm methanolic extract (0.25 mg/ml) did not block uptake of AgNPs (25 µg/ml) (Figure 3d). More NPs were found in cells exposed to 100 µg/ml of AgNPs compared with cells exposed to 25 µg/ml.

Induction of cytotoxicity, DNA SBs and oxidised base lesions (8-oxoG) by AgNPs

The Trypan blue exclusion assay showed no cytotoxic effect of AgNPs on HEK 293 cells after 30-min exposure. Cells exposed to 100 µg/ml AgNPs show a 48% decrease in proliferation activity (RGA assay) compared with the negative control (Figure 4). The CFA test showed a mild inhibition, with the

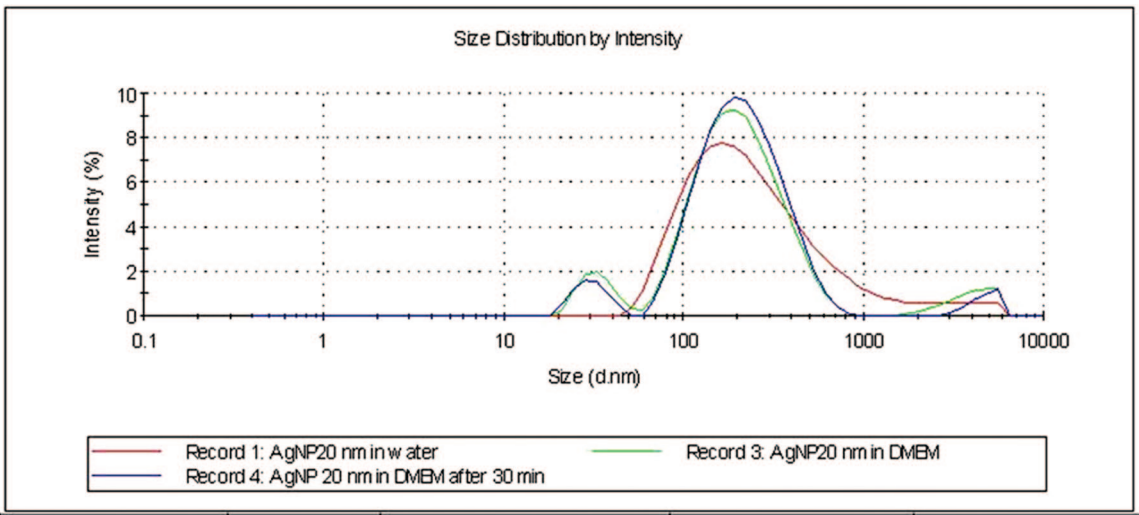

Sample name	Z-average (nm)	Small agglomorates/ singel particles (size, nm)		Medium agglomorates (size, nm)		Large agglomorates (size, nm)
		mean	peak	mean	peak	mean
AgNP 20 nm water	171			314	165	3761
AgNP 20 nm DMEM	153	33,9	32,6	226	190	4050
AgNP 20 nm DMEM after 30 min	157	30,8	28,2	231	190	4681

Fig. 1. DLS measurements of AgNPs in water and DMEM. The table shows the particle size as mean diameter (nm) and as peak where most particles occurred.

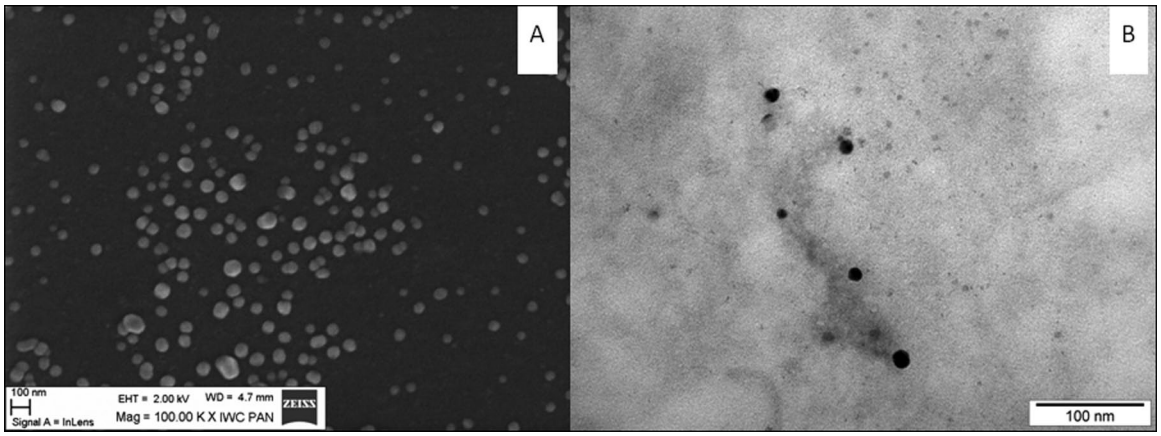

Fig. 2. Representative SEM (a) and TEM images of AgNPs (b).

highest concentration (100 µg/ml) causing a 21% decrease in the number of colonies.

The comet assay was used to determine the effect of AgNPs on HEK 293 cells after treatment with AgNPs. Both SBs and 8-oxoG (detected with hOGG1) were quantified. Positive control cells treated with H_2O_2 (250 µM) or Ro19-8022 plus visible light gave 63% and 45% tail DNA, respectively. We observed a dose-dependent increase of SBs after treatment of cells with AgNPs (Figure 4). Incubation with hOGG1 significantly increased tail intensity indicating that even the lowest AgNP concentration induced oxidised DNA lesions in addition to SBs.

Characterization of G. asclepiadea extracts

HPLC-DAD-MS analysis was carried out on methanolic (A1, B1) and aqueous (A2, B2) extracts from the flower (A1, A2) and haulm (B1, B2) of *G. asclepiadea* (Figure 5). Table 1 shows chromatographic, spectroscopic and spectrometric characteristics of the main phytochemicals present in the extracts such as swertiamarin, gentiopicroside, sweroside and isovitexin.

Effects of plant extracts on cells

We also studied potential cytotoxicity and genotoxicity of *G. asclepiadea* flower and haulm methanolic and aqueous extracts in HEK 293 cells. The CFA assay measures the number of colonies originating from single cells and thus detects viability. There was a stimulation of CFA by the lowest concentration of all extracts (0.25 mg/ml) and by 0.5 mg/ml and 2.5 mg/ml of the aqueous and methanolic haulm extracts. The highest concentration (25 mg/ml) of all extracts was cytotoxic and inhibited colony formation; the methanolic flower extract was especially potent (Figure 6).

The RGA assay confirmed the results obtained with the CFA assay. However, the lowest concentration (0.25 mg/ml) gave the maximum stimulation of RGA, and this was followed by a dose-dependent decline back to the control level, whereas the highest concentration (25 mg/ml) was cytotoxic and inhibited cell growth. The growth stimulation was most pronounced for the methanolic extracts (Figure 6).

Figure 6 also shows the DNA damage induced by *G. asclepiadea* extracts. Methanolic haulm extract caused the greatest increase in DNA SBs compared with the control, in particular at the two highest concentrations. Neither aqueous haulm and flower nor methanolic flower extracts exhibited significant genotoxicity.

Protective effect of G. asclepiadea extract against AgNP-induced DNA damage

The potential protective effect of plant extracts on AgNP-induced DNA damage was examined with the comet assay ± hOGG1. HEK 293 cells were pretreated with non-cytotoxic and non-genotoxic concentrations of *G. asclepiadea* flower extracts for 24 hours and with AgNPs for 30 min (Figures 7 and 8). Cells exposed to H_2O_2 (inducing 63% DNA in comet tails) or to Ro19-8022 plus light (inducing 45% DNA in comet tails) were used as positive controls. Pretreatment with 0.25 and 0.5 mg/ml of all the extracts (Figures 7a and 8a) protected DNA against SBs caused by AgNPs. This effect was not seen when cells were pretreated with the highest concentration (2.5 mg/ml) of extracts and with 1 µg/ml AgNPs. However, the same concentration of these extracts protected cells against DNA damage caused by either 25 µg/ml or 100 µg/ml of AgNPs (Figures 7a and 8a).

Figures 7b and 8b show the levels of 8-oxoG (net hOGG1-sensitive sites) in AgNP-treated cells. Cells pretreated with *Gentiana* extract show lower levels of 8-oxoG compared with cells that were not pretreated with the extract. Except for methanolic flower extract, all extracts protected cells against hOGG1-sensitive lesions induced by AgNPs. The fewest hOGG1-sensitive sites were detected after pretreatment of cells with methanolic haulm extract; thus, this extract exhibited the greatest protective effect.

Discussion

Nanomaterial safety and potential adverse health effects from exposure to nanomaterials are of great concern. It is therefore important to study candidate genotoxic NPs together with agents offering possible protective effects against such damage. Several studies have demonstrated that AgNPs are cytotoxic (21–23) and can promote oxidative stress (24,25). Recently, it was observed that AgNPs induced DNA damage. An increase in ROS levels was detected after 6-24 hours treatment with AgNPs, suggesting that oxidative stress might be an important mediator of cytotoxicity and genotoxicity (26,27).

We investigated whether AgNPs are able to enter the cells. TEM images show clearly that AgNPs are taken up by kidney

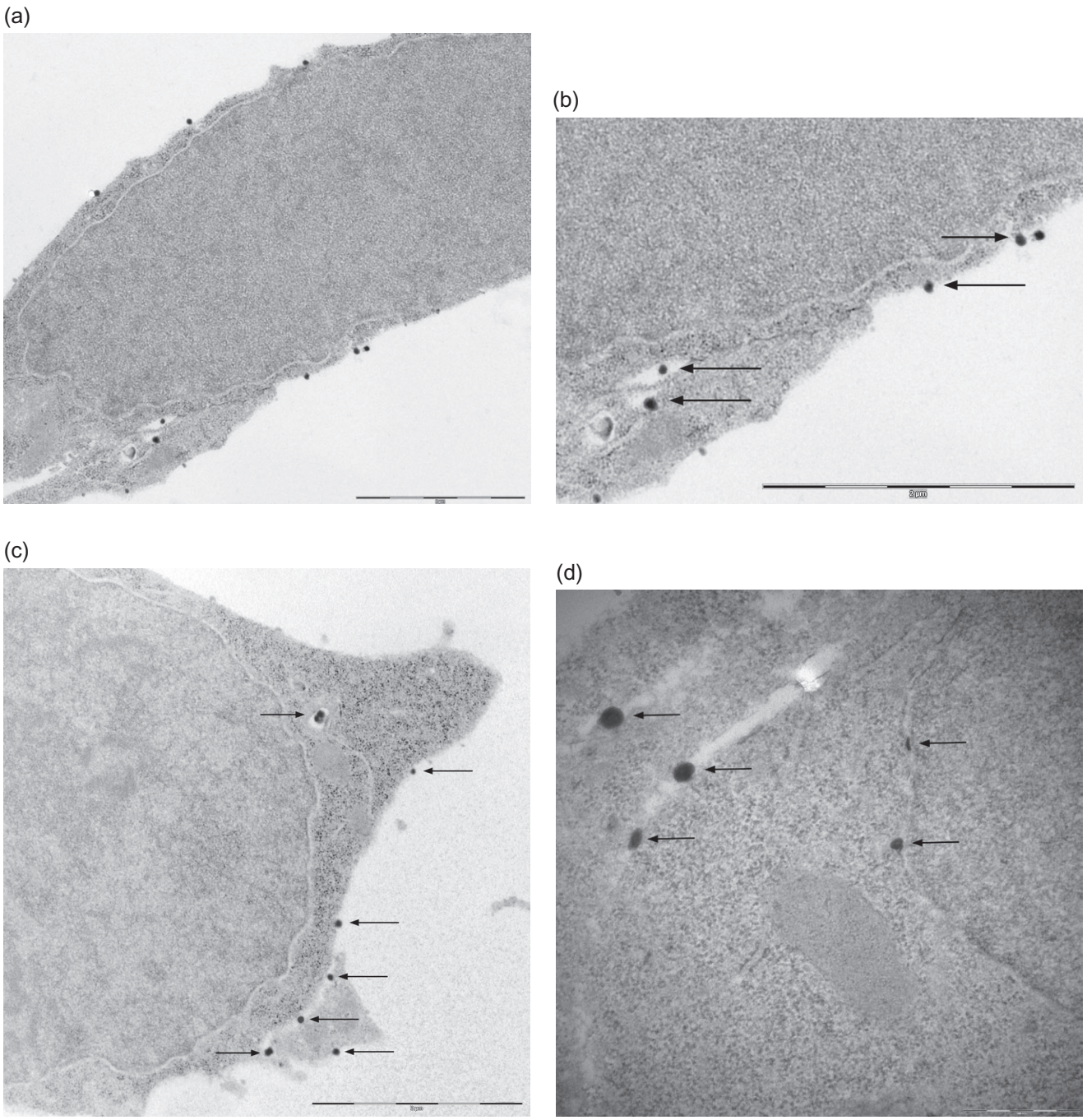

Fig. 3. Internalisation of AgNPs by HEK 293 cells. The cells were exposed to 25 and 100 µg/ml of AgNPs (20 nm) for 30 min, and intracellular and subcellular localisation was analysed by TEM. (a), (b), (c)—AgNPs 25 µg/ml; (d)—pretreatment with haulm methanolic extract (0.25 mg/ml) and treatment with AgNP (25 µg/ml); The arrows indicate NPs in the vacuoles and cytoplasm.

cells. They were found in vacuoles but also in cytoplasm (Figure 3). The same AgNPs (20 nm) were recently shown to be internalised by human epithelial lung A549, liver HepG2 and monocyte THP-1 cell lines (18). The authors detected AgNPs (20 nm) in vacuoles, cytoplasm and also in nucleus and mitochondria (18).

Cytotoxic effects of AgNPs were investigated using three distinct assays. The CFA assay is a true viability assay, measuring the ability of individual cells to survive and divide. RGA—reflecting the capacity of the cell population to proliferate—measures a mixture of cell killing and cycle delay. The TB exclusion assay simply detects membrane damage, which does not necessarily result in or indicate cell death. All three assays agree in showing no significant cytotoxicity up to 25 µg/ml. However, only the CFA & RGA assays demonstrated cytotoxicity over 25 µg/ml, whereas the TB assay did not.

Additionally, here we studied the impact of AgNPs on DNA damage in HEK 293 cells using the modified comet assay (19,28). To detect DNA oxidation, we used the specific human DNA repair enzyme hOGG1 that initiates base excision repair of 8-oxoG (13,29,30). Our experiments showed that AgNPs do

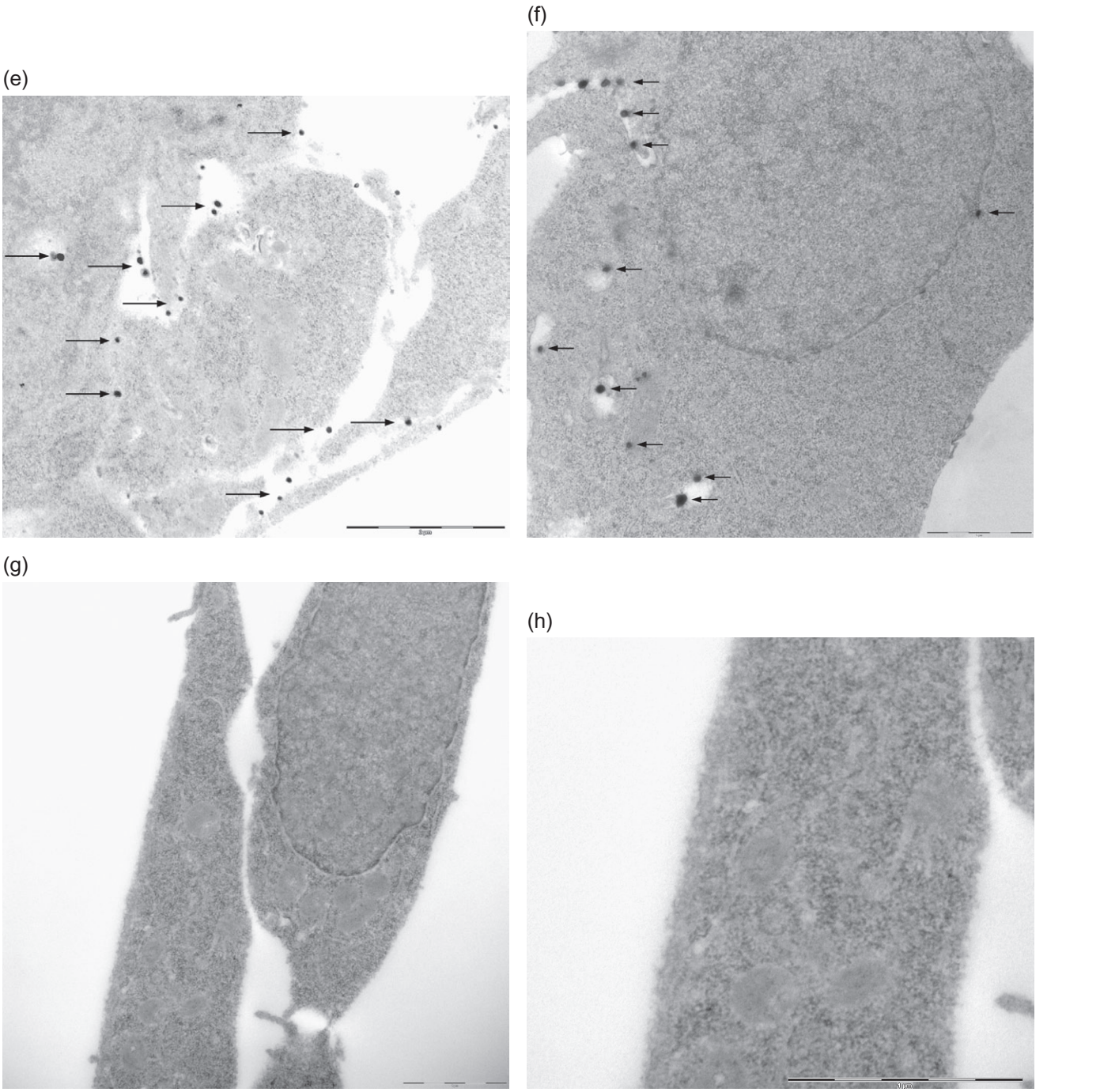

Fig. 3. Internalisation of AgNPs by HEK 293 cells. The cells were exposed to 25 and 100 µg/ml of AgNPs (20 nm) for 30 min, and intracellular and subcellular localisation was analysed by TEM. (e), (f)—AgNPs 100 µg/ml; (g), (h)—untreated cells. The arrows indicate NPs in the vacuoles and cytoplasm.

indeed induce this premutagenic DNA lesion. It should be noted that DNA oxidation is present at non-cytotoxic concentrations of AgNPs, confirming that this is a direct genotoxic effect.

Plant extracts from *Gentianaceae* species have been shown to have protective effects on human health, and several biologically active compounds have been identified as possessing positive attributes such as antiarthritic, antibacterial, anticancer, antifungal, antioxidant, anticoagulant, antiviral, neuroprotective, antispasmodic, hepatoprotective, wound healing, immunomodulatory and insecticidal (15,31–33).

We previously assessed the ability of the plant extracts from *G. aspelgiacea* to scavenge 1,1-diphenyl-2-picrylhydrazyl and to protect DNA from H_2O_2 at non-cytotoxic and non-genotoxic concentrations (17,34,35). Here, we have characterised components of extracts from *G. asclepiadea*. The extract contains compounds identified as swertiamarin, loganic acid, luteolin-diglucoside, isovitexin-glucoside, mangiferin, swertiamarin, gentiopicroside and homoorientin (Table 1).

As these extracts exhibited promising antioxidant potential, we here examined whether the extracts might protect against

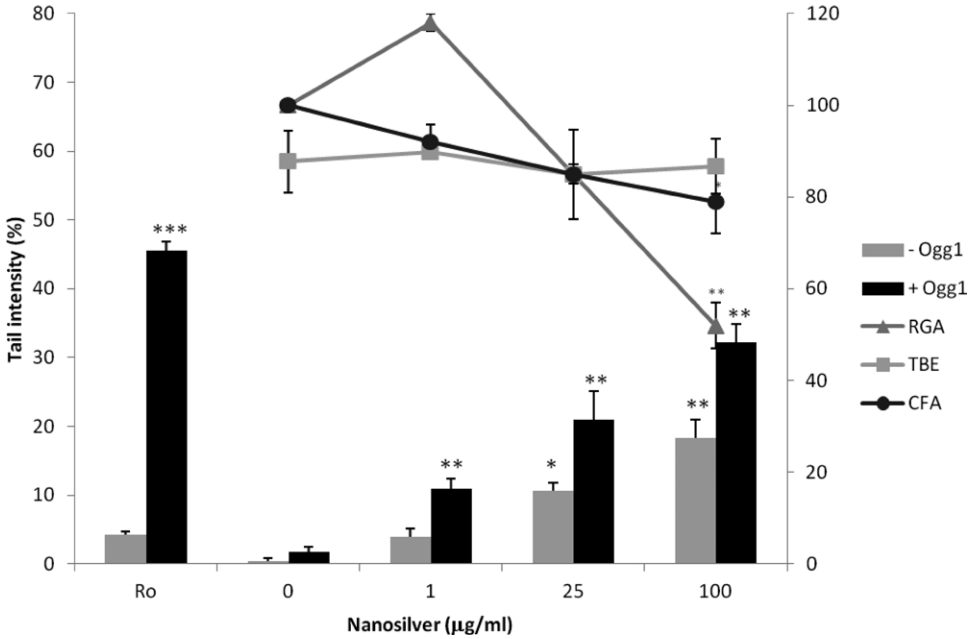

Fig. 4. Cytotoxicity and genotoxicity of AgNPs (30-min treatment) on HEK 293 cells. Trypan blue exclusion (TBE), RGA, CFA and DNA damage: SBs (−hOGG1) and SBs + 8-oxoG (+hOGG1). Cells treated with Ro19-8022 (1 µM) plus visible light were used as a positive control.

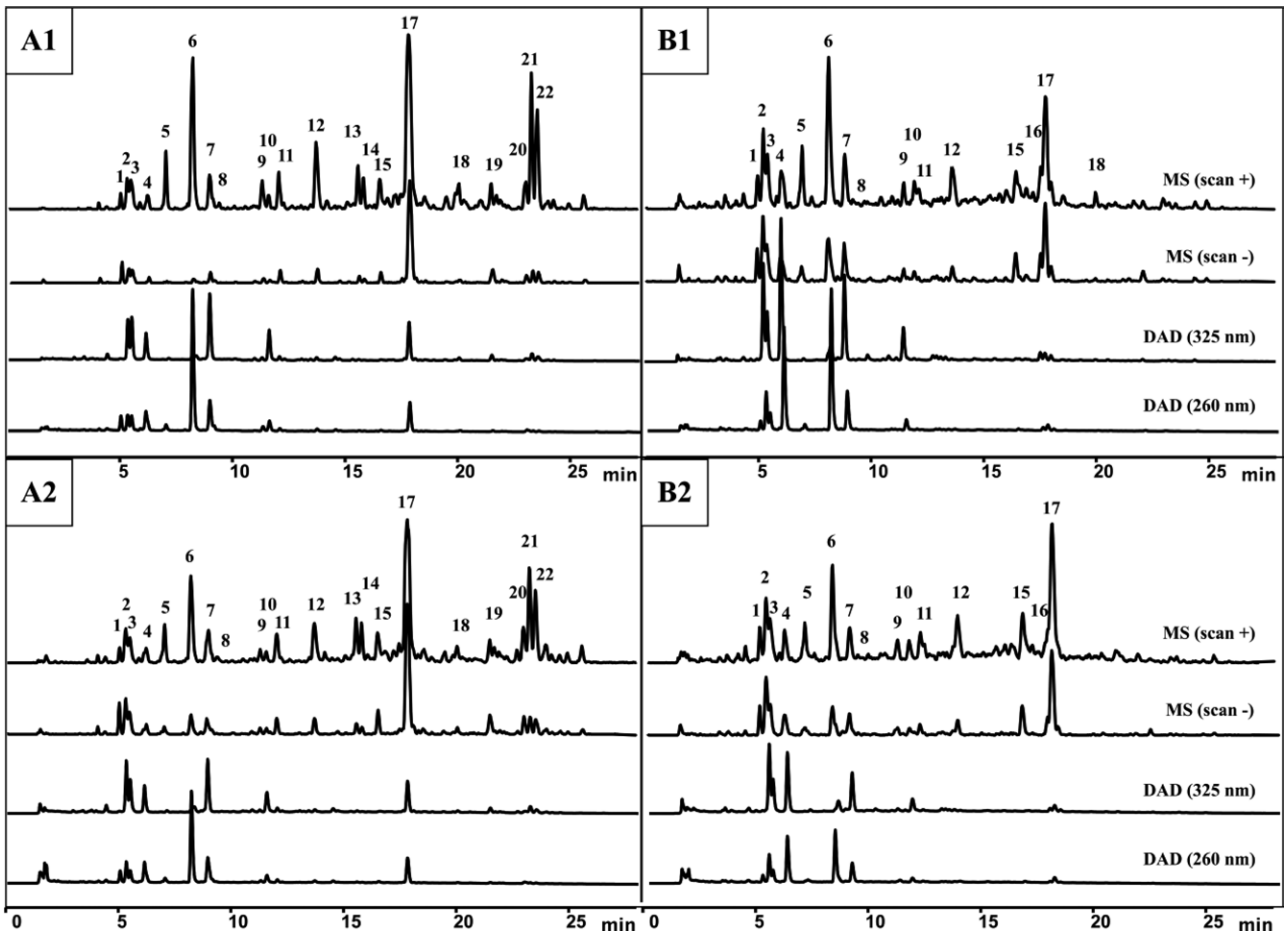

Fig. 5. HPLC-DAD-MS chromatograms of methanolic (A1, B1) and aqueous (A2, B2) extracts prepared from the flower (A1, A2) and haulm (B1, B2) of *G. asclepiadea*.

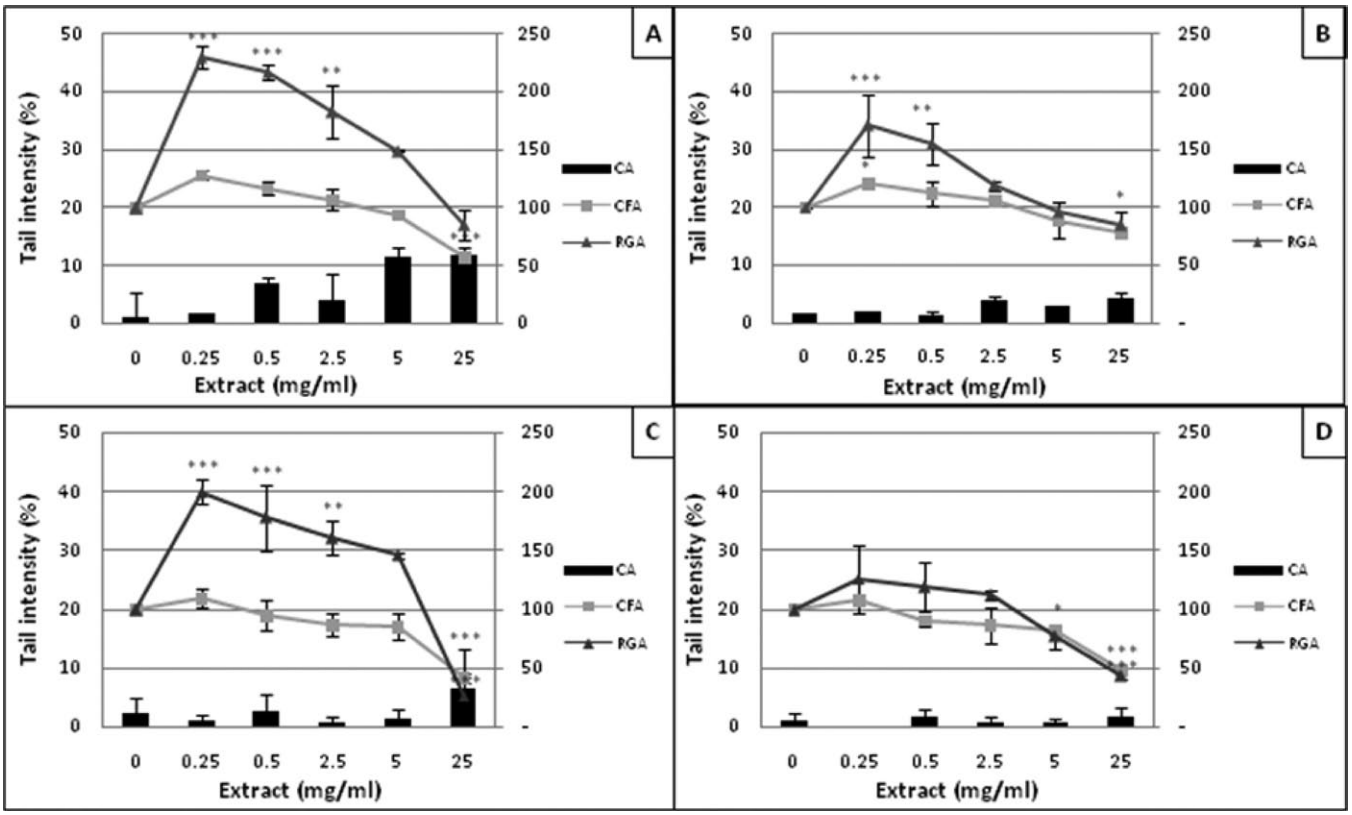

Fig. 6. Cytotoxicity and genotoxicity of *G. asclepiadea* extracts on HEK 293 cells after 24-hour treatment. DNA damage measured by the comet assay (CA); CFA and RGA. Extracts: (A)—methanolic haulm, (B)—aqueous haulm, (C)—methanolic flower, (D)—aqueous flower.

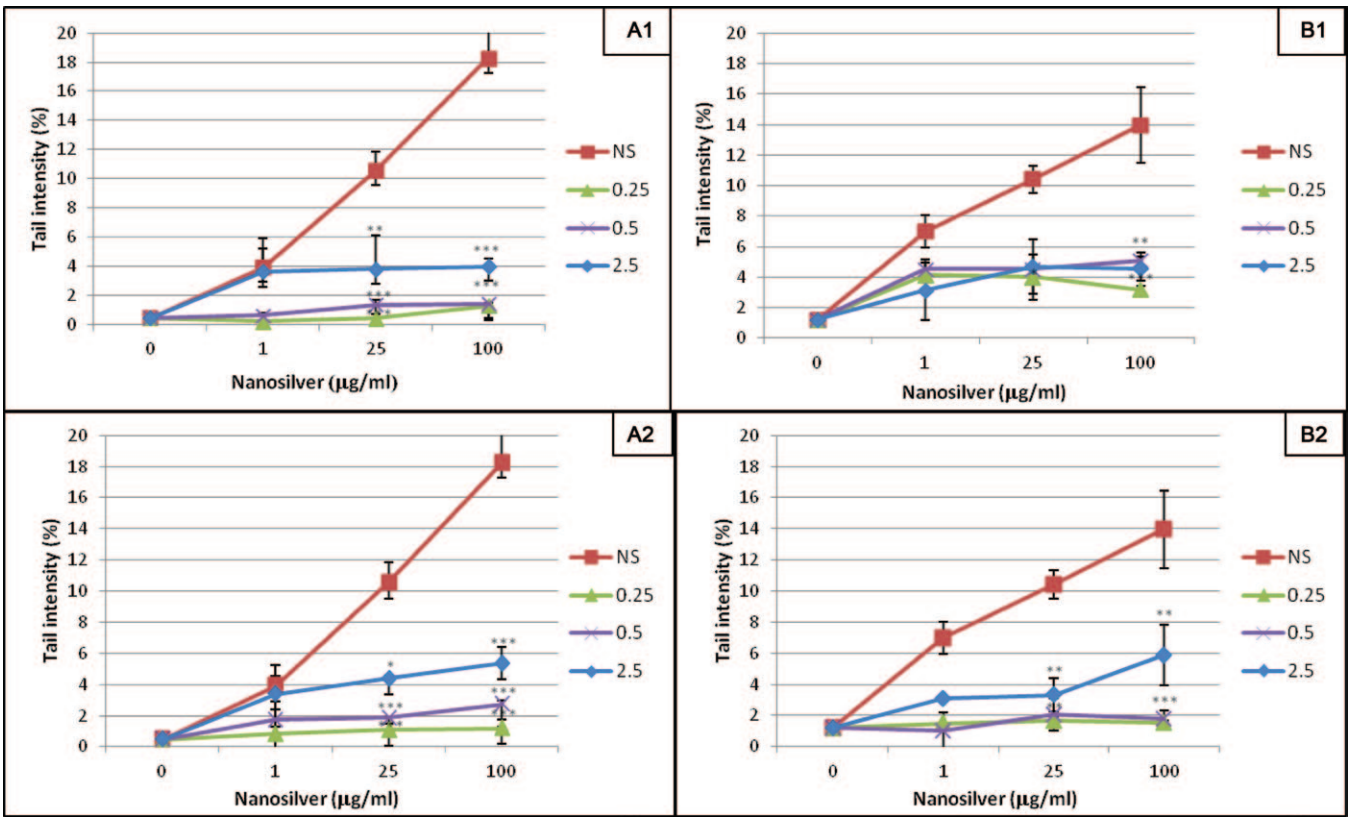

Fig. 7. The effect of 24-hour pretreatment with *G. asclepiadea* haulm extracts on DNA damage induced by AgNPs on HEK 293 cells. Cells were treated for 30 min with AgNPs, without pretreatment (NS) or pretreated for 24 hour with 0.25, 0.5 or 2.5 mg/ml of extracts. A1, B1—methanolic extract; A2, B2—aqueous extract. A1, A2—SBs; B1, B2—OGG1 lesions (8-oxo-G). Net hOGG1-sensitive sites were estimated by subtracting % tail DNA minus hOGG1 from % tail DNA plus hOGG1.

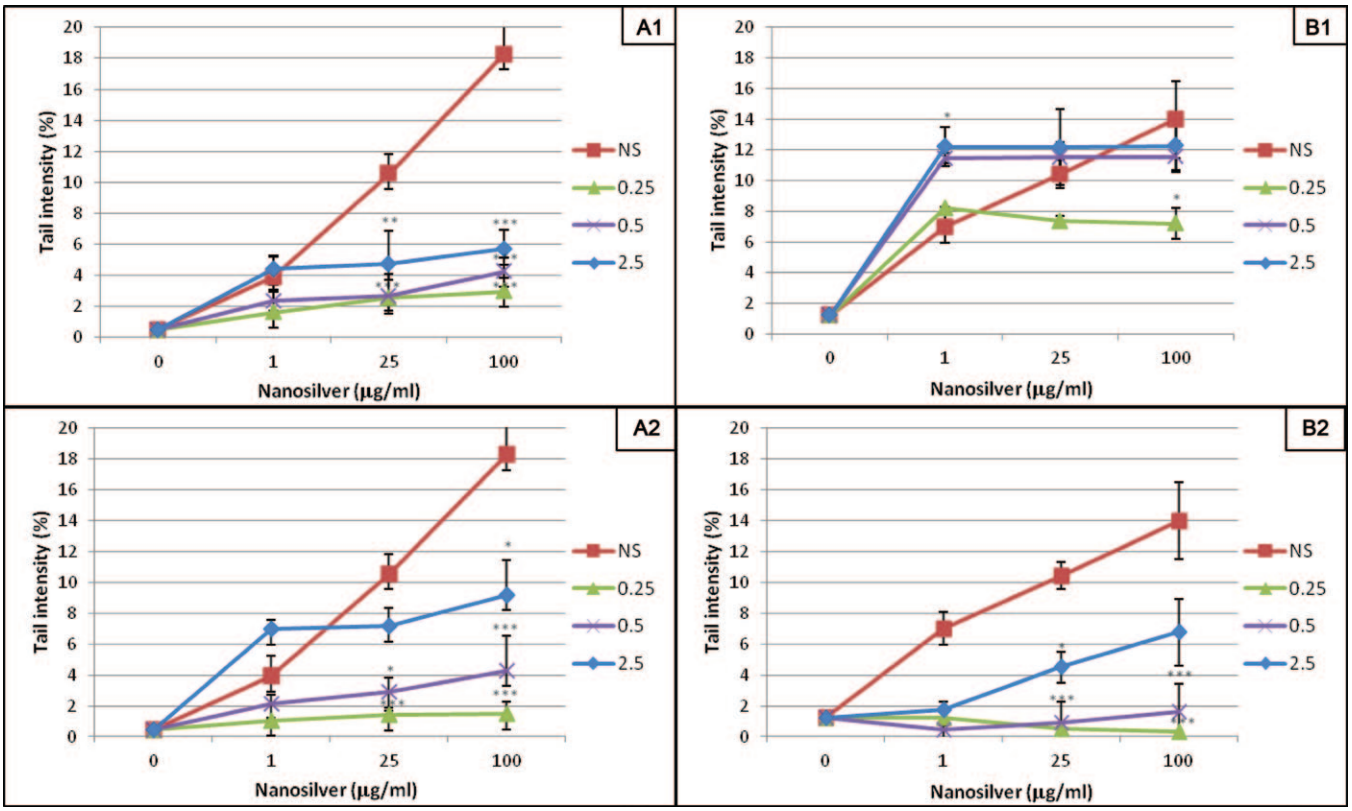

Fig. 8. The effect of 24-hour pretreatment with *G. asclepiadea* flower extracts on DNA damage induced by AgNPs on HEK 293 cells. Cells were treated for 30 min with AgNPs, without pretreatment (NS) or pretreated for 24 hour with 0.25, 0.5 or 2.5 mg/ml of extracts. A1, B1—methanolic extract, A2, B2—aqueous extract. A1, A2—SBs; B1, B2—OGG1 lesions (8-oxo-G) (hOGG1 sites estimated as in Figure 7).

Table I Chromatographic, spectroscopic and spectrometric characteristics of phytochemicals present in *G. asclepiadea* extracts

Peak	Rt (min)	λ_{max} (nm)	m/z (positive ionisation)	m/z (negative ionisation)	Mw	Molecular formula	Compound
1	5.0	250	399 $[M+Na]^+$	375 $[M-H]^-$	376	$C_{16}H_{24}O_{10}$	Loganic acid
2	5.3	250, 270, 340	611 $[M+H]^+$	609 $[M-H]^-$	610	$C_{27}H_{30}O_{16}$	Luteolin-diglucoside
3	5.5	270, 325	595 $[M+H]^+$	593 $[M-H]^-$	594	$C_{27}H_{30}O_{15}$	Isovitexin-glucoside
4	6.1	260, 320, 370	423 $[M+H]^+$	421 $[M-H]^-$	422	$C_{19}H_{18}O_{11}$	Mangiferin
5	7	240	397 $[M+Na]^+$	419 $[M+HCOO]^-$	374	$C_{16}H_{22}O_{10}$	Swertiamarin
6	8.2	250, 270	379 $[M+Na]^+$	401 $[M+HCOO]^-$	356	$C_{16}H_{20}O_9$	Gentiopicroside
7	8.9	270, 350	449 $[M+H]^+$	447 $[M-H]^-$	448	$C_{21}H_{20}O_{11}$	Homoorientin
8	9.1	250	381 $[M+Na]^+$	403 $[M+HCOO]^-$	358	$C_{16}H_{22}O_9$	Sweroside
9	11.2	250	413 $[M+Na]^+$	435 $[M+HCOO]^-$	390	$C_{16}H_{24}O_{10}$	Eustomoside
10	11.6	270, 350	433 $[M+H]^+$	431 $[M-H]^-$	432	$C_{21}H_{20}O_{10}$	Isovitexin
11	12.0	250, 325	697 $[M+Na]^+$	673 $[M-H]^-$	674	$C_{29}H_{38}O_{18}$	Gentiournoside D
12	13.7	250, 325	603 $[M+H]^+$	601 $[M-H]^-$	602	$C_{29}H_{30}O_{14}$	Amaroswerin
13	15.2	250, 310	873 $[M+Na]^+$	849 $[M-H]^-$	850	–	–
14	15.5	250, 310	873 $[M+Na]^+$	849 $[M-H]^-$	850	–	–
15	16.5	250, 325	577 $[M+Na]^+$	553 $[M-H]^-$	554	–	–
16	17.6	270, 325	779 $[M+H]^+$	777 $[M-H]^-$	778	–	–
17	17.8	250, 325	711 $[M+Na]^+$	687 $[M-H]^-$	688	$C_{30}H_{40}O_{18}$	Depressin
18	19.9	250, 310	547 $[M+Na]^+$	523 $[M-H]^-$	524	–	–
19	21.4	250, 325	575 $[M+Na]^+$	551 $[M-H]^-$	552	$C_{25}H_{28}O_{14}$	Gentioside
20	22.9	250, 325	549 $[M+Na]^+$	525 $[M-H]^-$	526	–	–
21	23.2	250, 325	857 $[M+Na]^+$	833 $[M-H]^-$	834	–	–
22	23.5	250, 325	857 $[M+Na]^+$	833 $[M-H]^-$	834	–	–

AgNP-induced DNA oxidation. The altered base 8-oxoG is important since it is highly mutagenic and thus potentially carcinogenic. *G. asclepiadea* extracts completely inhibited or decreased the induction of 8-oxoG by AgNPs. Methanolic haulm extract appeared as the most and the methanolic flower extract as the least potent in preventing 8-oxoG formation. Recently, we found that mangiferin displayed the strongest antioxidant potential among identified phytochemicals in *G. asclepiadea* extracts (35). In comparison with earlier data concerning antioxidant activities of phenolic compounds, the activity of mangiferin is comparable with that of rutin, commonly used as an antioxidant for medical purposes (36). It was also revealed that mangiferin had potent cytoprotective and antigenotoxic effects (37,38). Also the compounds homoorientin and

swertiamarine were found to possess significant antioxidant properties (39–41).

Antioxidants can exert their effects via direct mechanisms, by scavenging ROS, or they can enhance endogenous defence via indirect mechanisms, such as the induction of genes encoding antioxidant proteins (42). A free radical scavenging activity was observed in *G. decumbens* and *G. lutea* extracts (43,44). It is likely that the antioxidant potential of the extracts is driven by the bioactive compounds through both direct and indirect mechanisms. However, careful consideration of dose range is needed. Our extracts show protective effects against AgNP-induced DNA damage at low to moderate dose range, whereas at the highest dose both induction of damage and protection against DNA damage are seen. Protective doses did not induce cytotoxicity or genotoxicity although there was marked stimulation of proliferation. In accordance with our data, Ozturk *et al.* (44). showed the wound-healing property of *G. lutea* through the stimulation of mitotic activity and collagen production in chicken embryonic fibroblasts. The proliferative effect was also observed in splenocytes exposed to secoiridoids, the most common constituents of genus *Gentiana* (32,44) and in normal keratinocytes exposed to the flavonoid luteolin (45). In contrast, antiproliferative activity and apoptosis induced by *G. triflora* extract or luteolin on tumour cells were reported (14,45). Underlying this difference might be variations in organisation of signalling proteins between normal and cancer cells. The total bioactivity might also depend on synergistic and redox interactions among different molecules present in particular extracts.

Inhibition of uptake of AgNPs is unlikely to explain the protective effects of the *Gentiana* extracts as we have detected AgNPs inside cells in the presence of extract (Figure 3d).

Conclusion

In conclusion, our results clearly show that AgNPs are internalised by human kidney cells and localised mostly in vacuoles. We also show that AgNPs induce oxidative DNA damage in cells and that this damage could be counteracted by pretreatment with bioactive compounds. Specifically we measured formation of the potentially mutagenic oxidised DNA base 8-oxoG, and we demonstrate that this damage was significantly lowered by pretreatment with the plant extracts. Both by direct measurement of 8-oxoG and by showing the suppression of damage by known antioxidant phytochemicals, we give strong support to the hypothesis that oxidative stress underlies the toxicity of AgNP.

Our results imply that extracts of *G. asclepiadea* could have considerable medical relevance, as they could counteract formation of 8-oxoG and thus reduce mutagenicity and carcinogenicity that potentially can be induced also by AgNPs.

Funding

This work was supported by an EEA Polish-Norwegian research grant (PNRF-122-AI-1/07); Internal NILU grant (106170); VEGA grants of Ministry of Education, Science, Research and Sport of the Slovak Republic and Slovak Academy of Sciences (1/0025/11, 2/0072/09); APVT (20-00-2604); granted by governmental scholarships (1253/2009) and Tatra bank foundation.

Acknowledgements

We would like to thank Fridrich Gregáň and Dagmar Vaculčíková (Department of Chemistry, Faculty of Natural Sciences, Matej Bel University, Banská Bystrica, Slovakia) for providing us the *Gentiana asclepiadea* extracts. We also thank Kristi Henjum and Finn Bjørklid for their help with samples processing for TEM. Ro 19-8022 was a generous gift from Hoffmann La Roche.

Conflict of interest statement: None declared.

References

1. Salata, O. V. (2004) Applications of nanoparticles in biology and medicine. *J. Nanobiotechnol.*, **2**, 3–9.
2. SCENIHR. (2007) *Scientific Committee on Emerging and Newly-Identified HealthRisks: The Existing and Proposed Definitions Relating to Products of Nanotechnologies.*
3. Imasaka, K., Kanatake, Y., Ohshiro, Y., Suehiro, J. and Harashima, H. (2006) Production of carbon nanoonions and nanotubes using an intermittent discharge in water. *Thin Solid Films*, **506**, 250–254.
4. Warner, J. H., Ito, Y., Zaka, M. *et al.* (2008) Rotating fullerene chains in carbon nanopeapods. *Nano. Lett.*, **8**, 2328–2335.
5. Dandekar, P., Dhumal, R., Jain, R., Tiwari, D., Vanage, G. and Patravale, V. (2010) Toxicological evaluation of pH-sensitive nanoparticles of curcumin: acute, sub-acute and genotoxicity studies. *Food Chem. Toxicol.*, **48**, 2073–2089.
6. Singh, N., Manshian, B., Jenkins, G. J. S., Griffiths, S. M., Williams, P. M., Maffeis, T. G. G., Wright, C. H. J. and Doak, S. H. (2009) NanoGenotoxicology: the DNA damaging potential of engineered nanomaterials. *Biomaterials*, **30**, 3891–3914.
7. Henig, R. M. (2007) Our silver-coated future. OnEarth, **Fall**, 22–29.
8. Melayie, A., Sun, Z., Hindi, K., Milsted, A., Ely, D., Reneker, D. H., Tessier, C. A. and Youngs, W. J. (2005) Silver(I)-imidazole cyclophane gem-diol complexes encapsulated by electrospun tecophilic nanofibers: formation of nanosilver particles and antimicrobial activity. *J. Am. Chem. Soc.*, **127**, 2285–2291.
9. Margaret, I. P., Lui, S. L., Poon, V. K., Lung, I. and Burd, A. (2006) Antimicrobial activities of silver dressings: an in vitro comparison. *J. Med. Microbiol.*, **55**, 59–63.
10. Vigneshawaran, N., Kathe, A. A., Varadarajan, P. V., Nachane, R. P. and Balasubramanya, R. H. (2007) Functional finishing of cotton fabrics using silver nanoparticles. *J. Nanosci. Nanotechnol.*, **7**, 1893–1897.
11. Foldbjerg, R., Olesen, P., Hougaard, M., Dang, D. A., Hoffmann, H. J. and Autrup, H. (2009) PVP-coated silver nanoparticles and silver ions induce reactive oxygen species, apoptosis and necrosis in THP-1 monocytes. *Toxicol. Lett.*, **190**, 156–162.
12. Nel, A., Xia, T., Madler, L. and Li, N. (2006) Toxic potential of materials at the nanolevel. *Science*, **311**, 622–627.
13. Vidal, A. E., Hickson, I. D., Boiteux, I. and Radicella, J. P. (2001) Mechanism of stimulation of the DNA glycosylase activity of hOGG1 by the major human AP endonuclease: bypass of the AP lyase activity step. *Nucleic Acids Res.*, **29**, 1285–1292.
14. Matsukawa, K., Ogata, M., Hikage, T. *et al.* (2006) Antiproliferative activity of root extract from Gentian plant (*Gentiana triflora*) on cultured and implanted tumor cells. *Biosci. Biotechnol. Biochem.*, **70**, 1046–1048.
15. Georgieva, E., Handjieva, N., Popov, S. and Evstatieva, L. (2005) Comparative analysis of the volatiles from flowers and leaves of three *Gentiana* species. *Biochem. Syst. Ecol.*, **33**, 938–947.
16. Saric, M. (1989) Medicinal plants of SR Serbia, SASA, Belgrade, **9**, 278 (in Serbian).
17. Hudecova, A., Hasplova, K., Miadokova, E. *et al.* (2012) *Gentiana asclepiadea* protects human cells against oxidation DNA lesions. *Cell Biochem. Funct.*, **30**, 101–107.
18. Lankoff, A., Sandberg, W. J., Wegierek-Ciuk, A. *et al.* (2012) The effect of agglomeration state of silver and titanium dioxide nanoparticles on cellular response of HepG2, A549 and THP-1 cells. *Toxicol Lett.*, **208**, 197–213.
19. Collins, A., Dusinska, M., Gedik, A. C. and Stetina, R. (1996) Oxidative damage to DNA: do we have a reliable biomarker? *Environ. Health Perspect.*, **104**, 465–469.
20. Collins, A. and Dusinska, M. (2009) Application of the comet assay in human monitoring. In Dhawan, A., Anderson, D. (eds), *The Comet Assay in Toxicology*. Royal Society of Chemistry, Cambridge, pp. 201–221.
21. Ahamed, M., Karns, M., Goodson, M., Rowe, J., Hussain, S. M., Schlager, J. J. and Hong, Y. (2008) DNA damage response to different surface chemistry of silver nanoparticles in mammalian cells. *Toxicol. Appl. Pharmacol.*, **233**, 404–410.

22. Hsin, Y. H., Chen, C. H. F., Huang, S., Shih, T. S., Lai, P. S. and Chueh, P. J. (2008) The apoptic effect of nanosilver is mediated by ROS- and JNK-dependent mechanism involving the mitochondrial pathway in NIH3T3 cells. *Toxicol. Lett.*, **179**, 130–139.
23. Shin, S. H., Ye, M. K., Kim, S. H. and Kang, H. S. (2007) The effects of nano-silver on the proliferation and cytokine expression by peripheral blood mononuclear cells. *Int. Immunophramacol.*, **7**, 1813–1818.
24. Cha, K., Wong, H. W., Choi, Y. G., Lee, M. J., Park, J. H., Chae, H. K., Ryu, G. and Myung, H. (2008) Comparison of acute responses of mice livers to short-term exposure to nano-sized or micro-sized silver particles. *Biotechnol. Lett.*, **30**, 1893–1899.
25. Hussain, S. M., Hess, K. L., Gearhart, J. M., Geiss, K. T. and Schlager, J. J. (2005) In vitro toxicity of nanoparticles in BRL 3A rat liver cells. *Toxicol. In Vitro*, **19**, 975–983.
26. Foldbjerg, R., Olesen, P., Hougaard, M., Dang, D. A., Hoffmann, H. J. and Autrup, H. (2009) PVP-coated silver nanoparticles and silver ions induce reactive oxygen species, apoptosis and necrosis in THP-1 monocytes. *Toxicol. Lett.*, **190**, 156–162.
27. Wojewodzka, M., Lankoff, A., Dusinska, M., Brunborg, G., Czerwinska, J., Iwanenko, T., Stepkowski, T., Szumiel, I. and Kruszewski, M. (2011) Treatment with silver nanoparticles delays repair of X-ray induced DNA damage in HepG2 cells. *Nukleoinka*, **56**, 29–33.
28. Dusinska, M. and Collins, A. (2008) The comet assay in human biomonitoring: gene–environment interactions. *Mutagenesis*, **23**, 191–205.
29. Bjøras, M., Luna, L., Johnsen, B., Hoff, E., Haug, T., Rognes, T. and Seeberg, E. (1997) Opposite base-dependent reactions of a human base excision repair enzyme on DNA containing 7,8-dihydro-8-oxoguanine and abasic sites. *EMBO J.*, **16**, 6314–6322.
30. Morland, I., Rolseth, V., Luna, L., Rognes, T., Bjøras, M. and Seeberg, E. (2002) Human DNA glycosylases of the bacterial Fpg/MutM superfamily: an alternative pathway for the repair of 8-oxoguanine and other oxidation products in DNA. *Nucleic Acids Res.*, **30**, 4926–4936.
31. Szucs, Z., Danos, B. and Nyiredy, S. (2002) Comparative analysis of the underground parts of *Gentiana* species by HPLC with diode-array and mass spectrometric detection. *Chromatographia*, **56**, 19–23.
32. Jiang, R. W., Wong, K. L., Chan, Y. M., Xu, H. X., But, P. P. H. and Shaw, P. C. H. (2005) Isolation of iridoid and secoiridoid glycosides and comparative study on *Radix gentianae* and related adulterants by HPLC analysis. *Phytochemistry*, **66**, 2674–2680.
33. Dinda, B., Debnath, S. and Harigaya, Y. (2007) Naturally occuring secoiridoids and bioactivity of naturally occuring iridoids and secoiridoids. A review, part 2. *Chem. Pharm. Bull.*, **55**, 689–728.
34. Hudecova, A., Hasplova, K., Miadokova, E., Magdolenova, Z., Rinna, A., Galova, E., Vaculcikova, D., Gregan, F. and Dusinska, M. (2010) Cytotoxic and genotoxic effect of methanolic flower extract from *Gentiana asclepiadea* on COS 1 cells. *Neuroendocrinol. Lett.*, **31**, 21–25.
35. Hudecova, A., Kusnierewicz, B., Hasplova, K., Huk, A., Magdolenova, Z., Miadokova, E., Galova, E. and Dusinska, M. (2012) *Gentiana asclepiadea* exerts antioxidant activity and enhances DNA repair of hydrogen peroxide- and silver nanoparticles-induced DNA damage. *Food Chem. Toxicol.*, **50**, 3352–3359.
36. Kusznierewicz, B., Piasek, A., Bartoszek, A. and Namieśnik, J. (2011) The optimisation of analytical parameters for routine profiling of antioxidants in complex mixtures by HPLC coupled post-column derivatisation. *Phytochem. Anal.*, **22**, 392–402.
37. Rao, B. S. S., Sreedevi, M. V. and Rao, B. N. (2011) Cytoprotective and antigenotoxic potential of Mangiferin, a glucosylxanthone against cadmium chloride induced toxicity in HepG2 cells. *Food Chem. Toxicol.*, **47**, 592–600.
38. Das, S., Rao, B. N. and Rao, B. S. S. (2011) Mangiferin attenuates methylmercury induced cytotoxicity against IMR-32, human neuroblastoma cells by the inhibition of oxidative stress and free radical scavenging potential. *Chem. Biol. Interact.*, **193**, 129–140.
39. Zeraik, M. L., Serteyn, D., Deby-Dupont, G., Wauters, J. N., Tits, M., Yariwake, J. H., Angenot, L. and Franck, T. (2011) Evaluation of the antioxidant activity of passion fruit (*Passiflora edulis* and *Passiflora alata*) extracts on stimulated neutrophils and myeloperoxidase activity assays. *Food Chem.*, **128**, 259–265.
40. Zielińska, D. and Zieliński, H. (2011) Antioxidant activity of flavone C-glucosides determined by updated analytical strategies. *Food Chem.*, **124**, 672–678.
41. Jaishree, V. and Badami, S. (2010) Antioxidant and hepatoprotective effect of swertiamarin from *Enicostemma axillare* against D-galactosamine induced acute liver damage in rats. *J. Ethnopharmacol.*, **130**, 103–106.
42. Ozono, R. (2006) New biotechnological methods to reduce oxidative stress in the cardiovascular system: focusing on the Bach1/heme oxygenase-1 pathway. *Curr. Pharm. Biotechnol.*, **7**, 87–93.
43. Kusar, A., Zupancic, A., Sentjurc, M. and Baricevic, D. (2006) Free radical scavenging activities of yellow gentian (*Gentiana lutea L.*) measured by electron spin resonance. *Hum. Exp. Toxicol.*, **25**, 599–604.
44. Ozturk, N., Korkmaz, Y., Ozturk, Y. and Husnu Can Baser, K. (2006) Effects of gentiopicroside, sweroside and swertiamarine, secoiridoids from gentian (*Gentiana lutea* ssp. *Symphyandra*), on cultured chicken embryonic fibroblasts. *Planta Med.*, **72**, 289–294.
45. Verschooten, L., Smaers, K., Kelst, S. V., Proby, C., Maes, D., Declercq, L., Agostinis, P. and Garmyn, M. (2010) The flavonoid luteolin increases the resistance of normal, but not malignant keratinocytes, against UVB-induced apoptosis. *J. Invest. Dermatol.*, **130**, 2277–2285.